

## Preparation of magnesium hydroxide by modifier-directed hydration and its effect on flame retardancy and mechanical properties of polypropylene

Mei Jia Wang, Li Mei Bai, Meng Ting Zhang, Yu Xin Ma, Liu Cheng Zhao, Shao Ying Li

College of Mining Engineering, North China University of Science and Technology, Tangshan 063210, China  
Collaborative Innovation Center of Green Development and Ecological Restoration of Mineral Resources, Tangshan 063210, China

Hebei province Key Laboratory of Mining Development and Security Technology, Tangshan 063210, China

Corresponding author: limeibai@126.com (Li Mei Bai)

**Abstract:** With the rapid development of the polymer materials industry and the improvement of people's environmental awareness, magnesium hydroxide has been widely used in polymer materials due to its high decomposition temperature, non-toxic smoke suppression, and the advantages of neutralizing harmful gases produced by polymer combustion. However, the conventional preparation methods of magnesium hydroxide exhibit several issues, including high hydrophilicity, elevated polarity, and limited compatibility with polymers. This research proposes an improved method by adding sodium stearate and KH560 modifier, controlling the rate of magnesium oxide and preparing magnesium hydroxide flame retardants using a modifier-directed hydration method. Various characterizations confirmed its morphology, particle size and structure. The magnesium hydroxide exhibits low polarity, small particle size, stable structure and excellent hydrophobicity (with a contact angle of 120.32°, and a free energy of 1.34mN/m). In parallel, the magnesium hydroxide/polypropylene composites demonstrate excellent flame retardancy (LOI of 25%, V-1 grade) and simultaneously enhance the dispersion of magnesium hydroxide within the polypropylene matrix, improving the material's toughness and strength.

**Keywords:** modifier, hydration preparation, magnesium hydroxide, polypropylene

### 1. Introduction

With the advancement of the modern polymer materials industry, plastics, synthetic rubber, and synthetic fibers have been increasingly used in various fields such as architecture, electrical and electronics, aerospace, and manufacturing (Mensah et al. 2022; Mohammed et al. 2022; Muiruri et al. 2023). However, due to their chemical composition and structure, these materials are primarily composed of carbon and hydrogen atoms, making them highly flammable. Flammability has become the main obstacle that restricts the use of polymer materials in various fields. Polypropylene (PP) has been widely used as an engineering polymer for decades, primarily because of its excellent mechanical properties. However, the use of PP has been limited due to its high flammability, especially in the cable and wire industry. The passage of an electric current generates joule heating, which poses a potential hazard to polymer coatings intended to prevent electric shock (Brostow et al. 2019).

Polymer fire suppression is usually achieved through two primary strategies used in the development of flame retardant (FR) polymer materials. One approach involves adding flame retardant additives, while the other involves chemically incorporating flame retardant elements or groups into the polymer structure. To date, blending flame retardant with polymers has been considered a simple and effective method to reduce the flammability of materials (He et al. 2020; Morgan et al. 2013). Generally, halogenated flame retardant release noxious gases, such as hydrogen chloride, hydrogen bromide, and other halides, as well as smoke, when they are exposed to heat. Additionally, high

temperatures can also cause flame retardant compounds to decompose into more toxic substances, such as dioxins and furan derivatives (Jeno et al. 2021). In recent years, halogen-free flame retardant, such as metal hydroxides, have been widely used to address the issue of toxicity. Some of these include aluminum trihydrate ( $\text{Al}(\text{OH})_3$ ) and magnesium hydroxide ( $\text{Mg}(\text{OH})_2$ ), which have been used as suitable substitutes for conventional flame retardant. When a polymer material containing  $\text{Mg}(\text{OH})_2$  and  $\text{Al}(\text{OH})_3$  is heated, the metal hydroxides decompose and absorb heat (Henri et al. 2020). This process is accompanied by the release of water and the absorption of heat, which significantly reduces the temperature of the burning polymer's surface. The presence of oxygen is diminished, resulting in a decrease in the rate of combustion. In addition, metal hydroxide facilitates the formation of a protective layer on the surface of the burning polymer, which reduces the release of combustible products into the gas phase and decreases the amount of smoke produced and its toxicity. Furthermore,  $\text{Mg}(\text{OH})_2$  exhibits higher heat resistance compared to  $\text{Al}(\text{OH})_3$ , as it can withstand temperatures up to  $300^\circ\text{C}$ , whereas  $\text{Al}(\text{OH})_3$  can only withstand temperatures up to  $230^\circ\text{C}$  (Nerea et al. 2019; Parida et al. 2022).  $\text{Mg}(\text{OH})_2$  is non-toxic and smoke-suppressant. It neutralizes acidic gas produced by combustion and provides reliable fire-resistant protection for polymer materials (Arzhakova et al. 2023). Therefore, the use of  $\text{Mg}(\text{OH})_2$  in the field of FR materials has garnered significant attention.

Traditional preparation methods of  $\text{Mg}(\text{OH})_2$ , such as the precipitation method (Pilarska et al. 2012) and hydrothermal method (Sierra-Fernandez et al. 2014), often result in its strong polarity and hydrophilicity. This leads to the particles easily agglomerating and having poor compatibility with polymers. In addition, to ensure flame retardancy, it is necessary to fill the polymer with  $\text{Mg}(\text{OH})_2$  up to 60 wt% or more. However, this often results in a significant reduction in the polymer's processability and toughness (Zhang et al. 2018; Liang 2017; Wang et al. 2023). In light of these challenges, surface modification with various chemical groups is an effective strategy for optimizing the dispersion and compatibility of the filler particles in a polymer matrix (Zhang et al. 2020). For example, the dispersion and lipophilicity of  $\text{Mg}(\text{OH})_2$  can be optimized by utilizing the hydrophobicity of fatty acids and the silicophilic and oxygenophilic groups of silane coupling agents (Liu et al. 2019). Pang improved the compatibility of  $\text{Mg}(\text{OH})_2$  and the polymer by reacting lauric acid with  $\text{Mg}(\text{OH})_2$  to generate a Mg-C-O chemical bond (Pang et al. 2008). Tang prepared hydrophobic and well-dispersed  $\text{Mg}(\text{OH})_2$  using oleic acid as a surface modifier (Tang et al. 2011). Yuan used wet-modified the surface of  $\text{Mg}(\text{OH})_2$  with trimethoxy [3-(phenylamino) propyl] silane and found that the dispersion and lipophilicity of the modified  $\text{Mg}(\text{OH})_2$  were significantly improved (Yuan et al. 2010). Lan used vinyl triethoxysilane to modify the surface of  $\text{Mg}(\text{OH})_2$  through a drying process. It was observed that the modified  $\text{Mg}(\text{OH})_2$  particles underwent a transition from hydrophilic to hydrophobic, resulting in improved dispersion and less aggregation (Lan et al. 2016).

These studies all demonstrate that the surface properties of  $\text{Mg}(\text{OH})_2$  can be controlled to significantly improve its compatibility with polymers. This improvement in compatibility ultimately enhances its effectiveness as a flame retardant. However, most of the methods require the addition of numerous modifiers, which complicates the process and increases the risk of impurity formation. Based on this, a new method is proposed for preparing  $\text{Mg}(\text{OH})_2$  flame retardant using the modifier-directed hydration method to address the aforementioned issues. In this method, active magnesium oxide was used as the raw material. Sodium stearate and KH560 modifier were added separately to the solution during ultrasonic cavitation. The properties of the resulting  $\text{Mg}(\text{OH})_2$  were then compared. It can control the morphology of particles and optimize their dispersion during the hydration process, eliminating the need for additional crystal stabilizers. This reduces impurities and saves costs. In addition, this method significantly improves the flame retardancy and tensile strength of composites made from sodium stearate-modified magnesium hydroxide/polypropylene composites. This development offers a new and effective flame retardant for polymer materials.

## 2. Materials and methods

### 2.1. Experimental materials

Active magnesium oxide was obtained by calcining low-grade magnesite from Xiuyan, Liaoning City, Hebei Province. The primary component of the raw material is  $\text{MgO}$ , with a content of 81.03%. It also contains minor amounts of  $\text{SiO}_2$  and  $\text{Cl}$ , as well as trace elements. Sodium stearate was purchased from

Shanghai Macklin Biochemical Technology Co., Ltd. KH560 was purchased from Jinan Xing Fei Long Chemical Co., Ltd. Anhydrous ethanol was purchased from Tianjin Yong Da Chemical Reagent Co., Ltd. Hydrochloric acid was purchased from Tianjin Kai Xin Chemical Co., Ltd. Magnesium hydroxide was purchased from Tianjin Zhi Yuan Chemical Reagent Co., Ltd, and polypropylene was provided by Li Chang Rong Chemical Industry Company.

The XRD patterns analysis is shown in Fig. 1. The XRD spectra show that active magnesium oxide exhibits no impurity peaks and has narrow characteristic diffraction peaks with high intensity, which indicates that MgO has a well-formed crystal structure, a large grain size, and high purity.

Table 1. Chemical composition of active magnesium oxide.

Composition	MgO	SiO <sub>2</sub>	SO <sub>3</sub>	Cl	K <sub>2</sub> O	CaO	Fe <sub>2</sub> O <sub>3</sub>	Pd
Wt/%	81.03	0.1	0.046	0.554	0.008	0.02	0.008	0.017

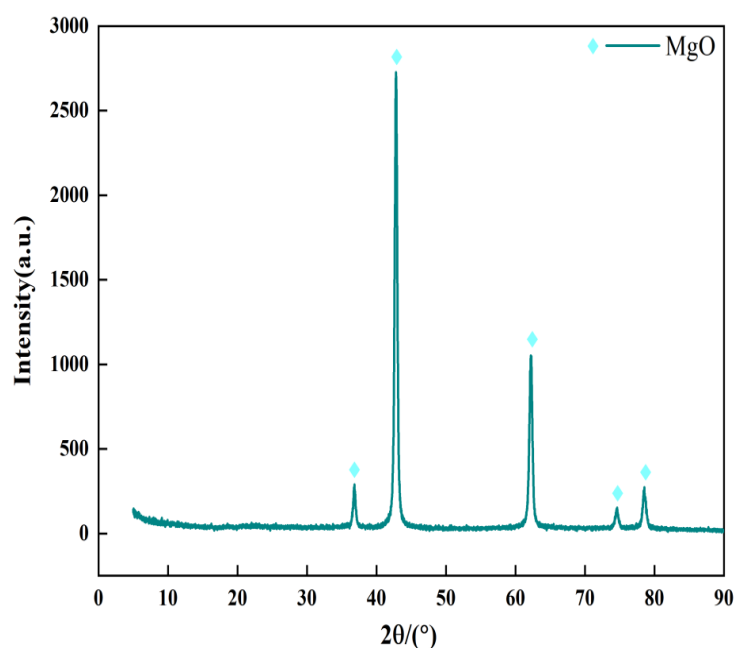


Fig. 1. XRD patterns of magnesium oxide

## 2.2. Hydration preparation process

Taken 0.067 g/mL of active magnesium oxide solution and stirred it thoroughly with a magnetic stirrer. Then, put the ultrasonic cleaner into the ultrasonic dispersion pre-treatment for 5 minutes (with an ultrasonic power of 100W) to obtain the magnesium oxide dispersion solution. Next, a beaker containing 400ml of deionized water was placed in an ultrasonic cleaner and heated to 80°C. A peristaltic pump was used to peristaltic the magnesium oxide dispersion into the beaker (ultrasonic power was 300W). Sodium stearate and KH560 modifier were added separately using a pipetting gun, with an additional amount of 3% (the mass fraction was calculated based on the percentage of the added amount of magnesium oxide). The mixture was continuously stirred and hydrated for two hours (Xing et al. 2018). After the reaction, the solution was cooled, pumped, filtered, and washed three times with water and anhydrous ethanol to avoid strong agglomeration. Finally, the cake was dried and ground, and the obtained magnesium hydroxide powder was used for subsequent detection and analysis. The experimental process is shown in Fig. 2.

## 2.3. Preparation of composite materials

Unmodified magnesium hydroxide, sodium stearate-modified magnesium hydroxide, KH560-modified magnesium hydroxide, and commercially available regular (AR) magnesium hydroxide were each uniformly stirred with polypropylene. The composite contained 40 wt% of magnesium hydroxide.

Subsequently, a micro twin-screw extruder was used for homogeneous extrusion, with the following temperature settings:

- Zone one controlled temperature at 200°C
- Zone two controlled temperature at 225°C
- Head zone one temperature at 200°C
- Head zone two temperature at 180°C

The extruded product was cooled and then pulverized. Finally, the samples were injected into an injection molding machine to form elongated strips with notches and dumbbell shapes, with an injection temperature used was 200°C. These samples were used to test the flame retardancy and mechanical properties to evaluate the effect of modifiers on the properties of magnesium hydroxide/polypropylene composite materials.

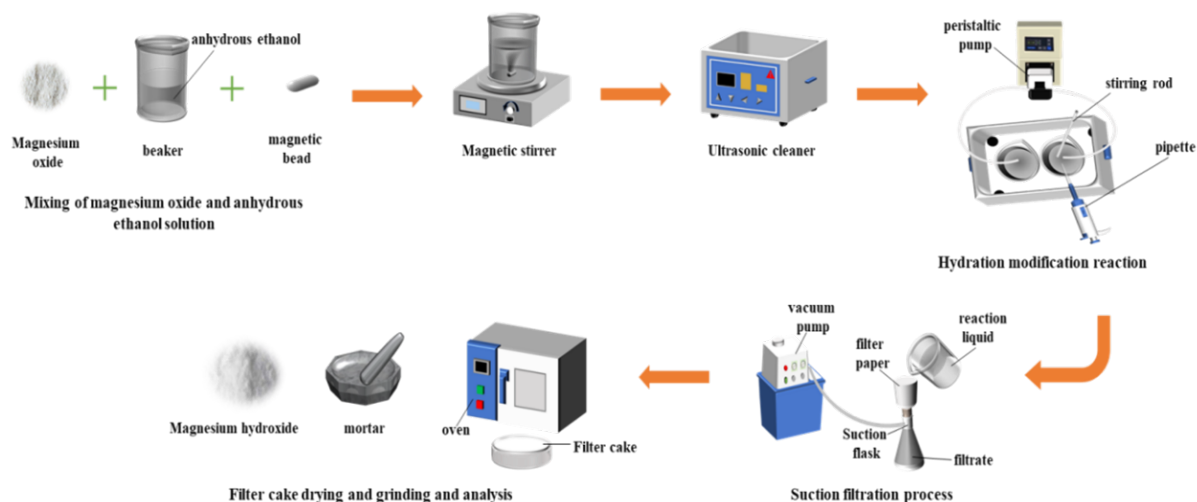


Fig. 2. Schematic diagram of experimental flow

## 2.4. Characterization of samples

X-ray diffractometer (model: D/MAX2500PC) produced by RIGAKU Corporation, Japan, was used for phase analysis. The instrument utilized Cu K $\alpha$  radiation ( $\lambda=1.54056\text{\AA}$ ) as the light source, with a scanning speed of  $10^\circ/\text{min}$  and an angular scanning range of  $10^\circ\text{-}80^\circ$ . Morphological analysis was performed using a scanning electron microscope (model: Scios) manufactured by FEI, Czech Republic, operating at an acceleration voltage of 10kV and magnifications ranging from 10,000 to 50,000. Peak shape variations were examined using an infrared spectrometer (model: VERTEX70) from Bruker, Germany, with a testing range of  $400\text{-}4000\text{cm}^{-1}$ . The contact angle measuring instrument (model: JY-PHB) produced by Chengde Youte Testing Instrument Manufacturing Co., Ltd. was used to test the samples for their affinity and hydrophobicity. Elemental analysis of the surface of pre-modified and post-modified magnesium hydroxide, X-ray photoelectron spectrometer (model: ESCALAB250Xi) produced by Thermo Fisher Scientific, USA, was employed. The surface element content of the magnesium hydroxide was determined. Thermal stability and component analysis were conducted using a simultaneous thermal analyzer (model: STA449F3-DSC200F3) from Netzsch, Germany, with a temperature range of  $25\text{-}700^\circ\text{C}$ . The cone calorimeter (model: Motis CCT) produced by Motis Combustion Technology Co., Ltd., with the sample size of  $100\times 100\times 3.0\text{mm}^3$  and the radiant power of  $35\text{kW}/\text{m}^2$ , was used to test the cone calorimeter of magnesium hydroxide before and after modification. Pyrolysis combustion flow calorimetric measurements (model: FTT), UK, with a temperature range of  $125\text{-}750^\circ\text{C}$  and the speed is  $1\text{K}/\text{s}$  to assess the flammability of the polymer. The Minimum Oxygen Index testing used an oxygen index tester (model: JF-3) manufactured by Beijing Xinsheng Zhuorui Technology Co., Ltd., China. Impact performance testing was done on notched samples using an impact tester (model: GLCJ-50) from Guoliang Instruments Co., Ltd., Wuhan, China. Tensile performance testing was performed on dumbbell-shaped samples using a universal tensile testing machine (model: WDW-20) from MTS Industrial Systems Co., Ltd.

### 3. Results and discussion

#### 3.1. Characterization of magnesium hydroxide prepared by hydration

To observe the microstructure of magnesium hydroxide before and after modification by SEM, as shown in Fig. 3. Fig. 3(a) shows that the unmodified magnesium hydroxide exhibits a clear outline and a regular hexagonal plate-like morphology with planar growth. Fig. 3(b) depicts the sodium stearate-modified magnesium hydroxide with a blurred outline, its shape transforms into smaller round disks with a smooth surface. Fig. 3(c) shows KH560-modified magnesium hydroxide, which still retains a hexagonal plate-like morphology. However, the plates are thinner and exhibit intertwined, aggregated growth. These results demonstrate that sodium stearate promotes the encapsulation of magnesium hydroxide particles by an organic polymer layer (Liu et al. 2012). At the same time, KH560 significantly affects the arrangement of magnesium hydroxide.

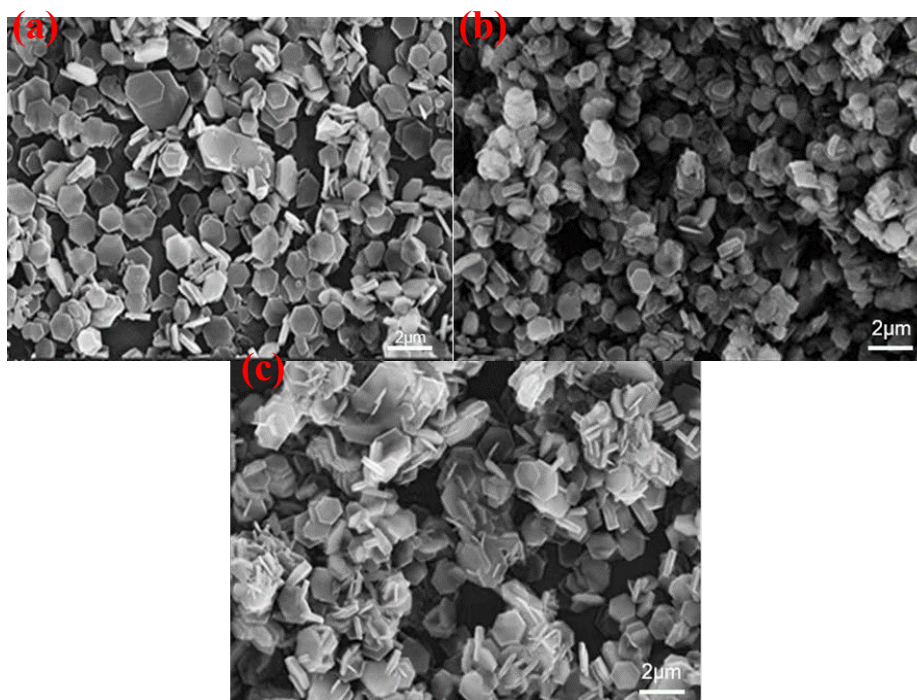


Fig. 3. SEM images of magnesium hydroxide before and after modification

Furthermore, by comparing the granulometry distribution curves in Fig. 4, it can be observed that the addition of the modifying agent causes the particle size distribution range of magnesium hydroxide to gradually shift to the left and exhibit a tendency towards a standard normal distribution. Specifically, unmodified magnesium hydroxide exhibits  $D_{50}=3.49\ \mu\text{m}$ , with particle sizes primarily distributed between  $1.25\ \mu\text{m}$  and  $14.28\ \mu\text{m}$ . This distribution demonstrates larger particle sizes that are consistent with the width dimensions of the flat hexagonal plate-like morphology. By contrast, sodium stearate-modified magnesium hydroxide exhibits  $D_{50}=2.66\ \mu\text{m}$ , with particle sizes primarily ranging between  $1.17\ \mu\text{m}$  and  $9.75\ \mu\text{m}$ . This indicates smaller particle sizes, suggesting that the addition of the modifier promotes surface reactions, inhibits the growth of magnesium hydroxide, and results in a nucleation rate more excellent than the growth rate, leading to a reduction in particle size. After modification with KH560, magnesium hydroxide's  $D_{50}=3.43\ \mu\text{m}$ , with particle range between  $1.32\ \mu\text{m}$  and  $14.33\ \mu\text{m}$ . Compared to unmodified magnesium hydroxide, the particle size and morphology remain consistent. It shows that the particle size of magnesium hydroxide, which has been modified with sodium stearate, is smaller and more uniform.

To further confirm the structure of the prepared samples, the XRD patterns of magnesium hydroxide before and after modification are presented in Fig. 5. The characteristic peak positions of sodium stearate-modified and KH560-modified magnesium hydroxide align with those of unmodified magnesium hydroxide, and no new characteristic peak appears, indicating that the addition of modifiers does not disrupt the crystal structure of magnesium hydroxide (Wang et al. 2023). The diffr-

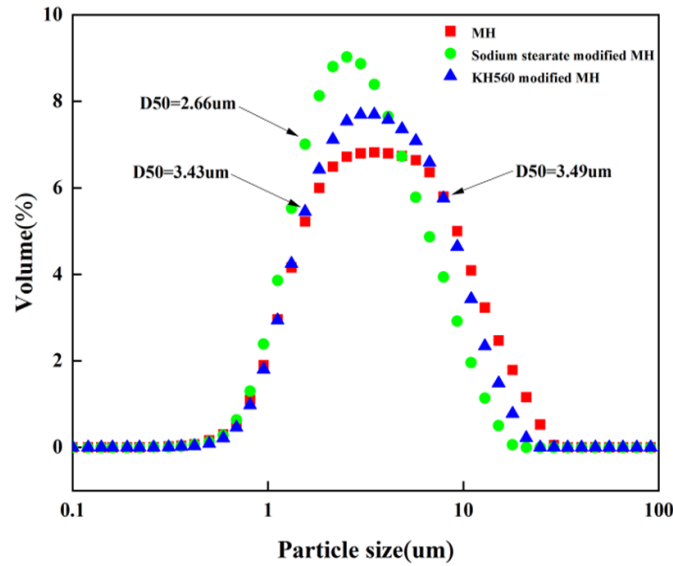


Fig. 4. Size distribution curves of magnesium hydroxide before and after modification

ction angles are  $18.49^\circ$ ,  $38^\circ$ ,  $50.77^\circ$ , and  $58.60^\circ$ , and there are strong characteristic peaks corresponding to (001), (101), (102), and (110) crystal planes of magnesium hydroxide, respectively. Among these, the (001) plane is non-polar, while the (101) plane is polar (Bhatt et al. 2021; Tang et al. 2020). The surface polarity of magnesium hydroxide can be characterized by the intensity ratio of the  $I_{001}$  and  $I_{101}$  diffraction peaks (Li et al. 2022; Mastronardo et al. 2017). With the addition of the sodium stearate modifier, the intensity ratio of the  $I_{001}/I_{101}$  peak increases. This indicates a decrease in the surface polarity of magnesium hydroxide after modification, which results in improved dispersion characteristics. Conversely, the peak intensity ratio of  $I_{001}/I_{101}$  decreases for KH560-modified magnesium hydroxide, indicating an increase in the polarity of magnesium hydroxide when it is modified with KH560. This could potentially hinder composite formation with polypropylene in the later phase.

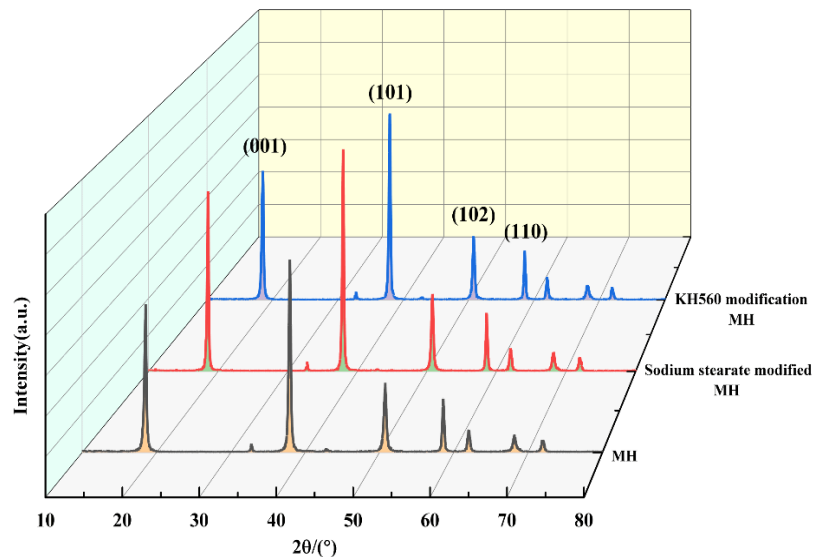


Fig. 5. XRD patterns of magnesium hydroxide before and after modification

### 3.2. Mechanism of action of modifier on magnesium hydroxide surface

Adding a modifier can significantly impact the surface free energy of magnesium hydroxide, resulting in distinct wettability and activity characteristics. Regarding wettability, a substance is considered hydrophobic if a water droplet does not readily adhere to the substrate and the contact angle is more than  $90^\circ$ . On the other hand, if the water droplet rapidly spreads on the substrate with a contact angle

of less than  $90^\circ$ , it signifies a hydrophilic material (Zahra et al. 2023). The contact angle in the unmodified magnesium hydroxide (refer to Fig. 6a) is  $38.39^\circ$ , indicating its hydrophilic nature, with a corresponding surface free energy of 17.34 mN/m. In contrast, sodium stearate-modified magnesium hydroxide (refer to Fig. 6b) exhibits a contact angle of  $120.32^\circ$ , and the surface free energy decreases to 1.34 mN/m. Magnesium hydroxide, modified with KH560 (refer to Fig. 6c), exhibits a contact angle of  $34.09^\circ$ , indicating an increased surface free energy of 18.21 mN/m. This finding further confirms the hydrophilic nature of the material. The stereoscopic effect of the changes in the contact angle before and after the modification of magnesium hydroxide is visually demonstrated in Fig. 6d. It is evident that the addition of the KH560 modifier did not successfully alter the surface properties of magnesium hydroxide, whereas the sodium stearate modifier effectively changed the surface properties of magnesium hydroxide, reducing its surface-free energy and transforming it into a hydrophobic material.

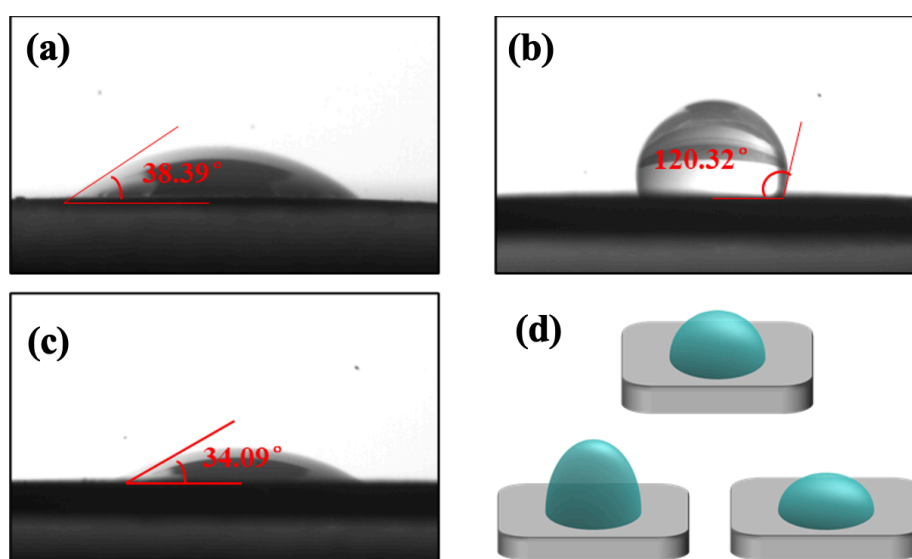


Fig. 6. Contact Angle of magnesium hydroxide before and after modification

During the hydration process of sodium stearate modifier, its molecules dissociate and react with the hydroxide ions in water to form stearic acid. The  $-\text{COOH}$  group of stearic acid interacts with the  $-\text{OH}$  group on the surface of magnesium hydroxide, thereby altering the surface properties of magnesium hydroxide. After modification, the hydrophilic  $-\text{OH}$  group is consumed, and the magnesium hydroxide is coated with a long carbon chain of stearic acid. At the other end of the stearic acid and magnesium hydroxide, there is a hydrophobic methyl group, which enhances its surface hydrophobicity. In the hydration process of the KH560 modifier, the modification of magnesium hydroxide involves the hydrolysis of its active group. The  $\text{Si-O-CH}_3$  group can be converted into  $\text{Si-OH}$ , which then forms a hydrogen bond with the  $\text{OH}$  group on the surface of magnesium hydroxide. This leads to a dehydration condensation reaction, resulting in the formation of a covalent bond (Zhang et al. 2023). KH560 contains a short carbon chain and a hydrophilic ester group.

Therefore, stearic acid-modified magnesium hydroxide exhibits good hydrophobicity. Fig. 7 illustrates the action mechanism of sodium stearate and KH560 in the hydration modification process.

Fig. 8 illustrates the infrared spectra of magnesium hydroxide before and after modification. According to the relevant spectroscopic analysis guidelines (Nyquist. 1998), the absorption peak observed at approximately  $3694\text{ cm}^{-1}$ , which is attributed to the  $\text{O-H}$  stretching vibration, provides additional evidence that the product is magnesium hydroxide (Ryo et al. 2021; Song et al. 2023). The band at  $3640\text{ cm}^{-1}$  is attributed to the presence of  $\text{O-H}$  groups (Guo et al. 2017), further indicating that the addition of sodium stearate and KH560 modifiers does not alter the formation of the hydration product. Compared to unmodified magnesium hydroxide, sodium stearate-modified magnesium hydroxide exhibits peaks at  $2916.76\text{ cm}^{-1}$  and  $2851.56\text{ cm}^{-1}$ , corresponding to the symmetric vibrations in  $-\text{CH}_2-$  and the asymmetric vibrations in  $-\text{CH}_3-$ . Both  $\text{ACH}_3$  and  $\text{ACH}_2-$  are derived from sodium stearate molecules, indicating successful adsorption of the sodium stearate molecules onto the surface of magne-

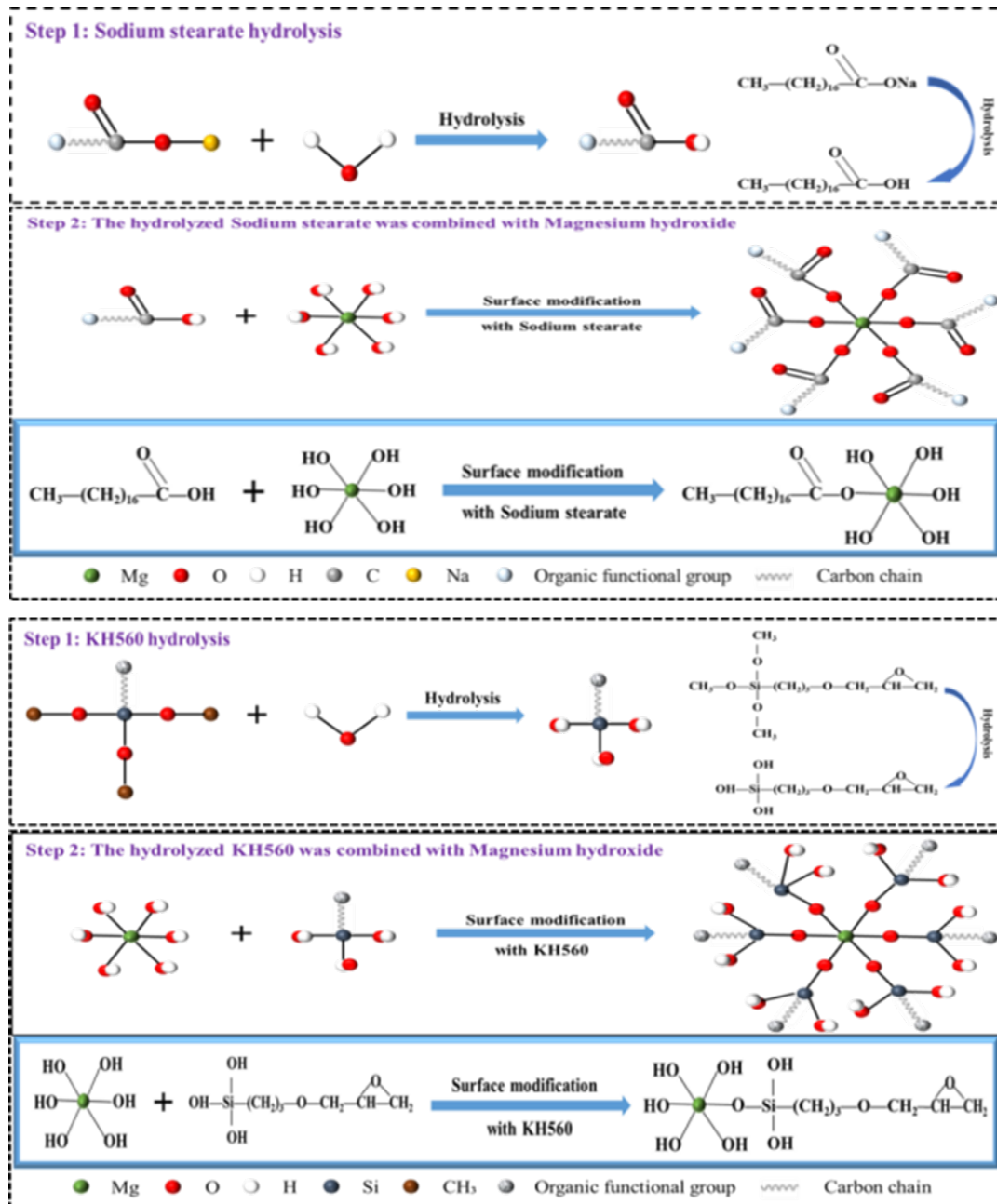


Fig. 7. Proposed bonding mechanism of sodium stearate and KH560 with magnesium hydroxide

sium hydroxide (Li et al. 2018). Furthermore, when KH560 is added after 60 minutes into the hydration process, the crystallization of magnesium hydroxide is complete with minimal lattice distortion and a slower reaction. As a result, only a limited amount of the modifier is attached to the surface of the magnesium hydroxide, which is why the absorption peak representing Si-O-C was not detected, as there were fewer adhesions.

XPS was used to analyze the chemical composition and valence states of elements in sodium stearate and KH560-modified magnesium hydroxide. In Fig. 9a's full spectrum, characteristic peaks for the Mg, O, C, and Si elements were detected. In the narrow scan XPS spectra (refer to Figs. 9b-e), the Mg1s spectrum (refer to Fig. 9b) shows peaks at 1304.83 eV and 1303.31 eV, which are higher than the standard binding energy at 1303.03 eV. This indicates a shift in the binding energy due to the addition of modifiers during the process of modifying hydration. In the C1s spectrum (refer to Fig. 9c), the peaks at 284.81 eV and 285.62 eV were higher than the standard binding energy at 284.78 eV, suggesting the presence of C-C bonds in alkyl groups (Li et al. 2021). This confirms the chemical bonding phenomena induced by the addition of modifiers to magnesium hydroxide. In the O1s spectrum (refer to Fig. 9d), peaks at 530.88



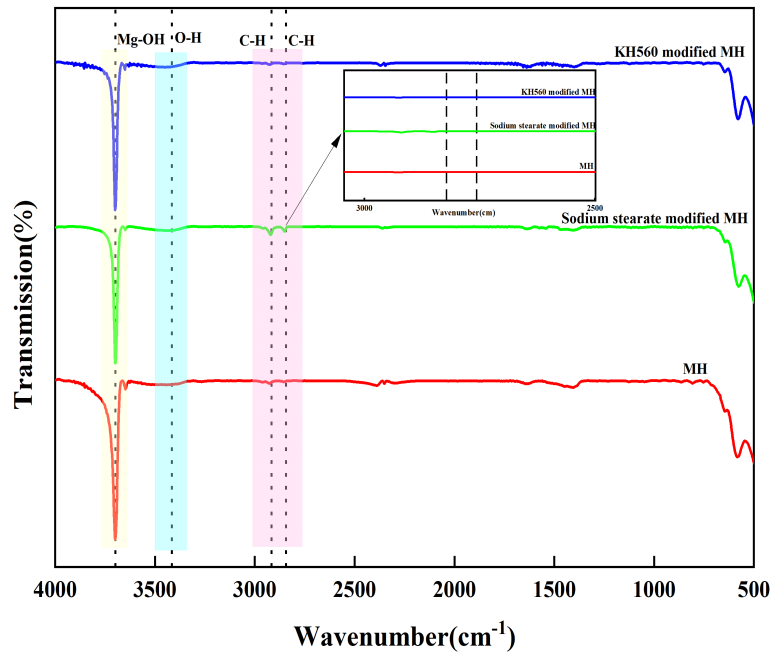


Fig. 8. Infrared spectra of magnesium hydroxide before and after modification

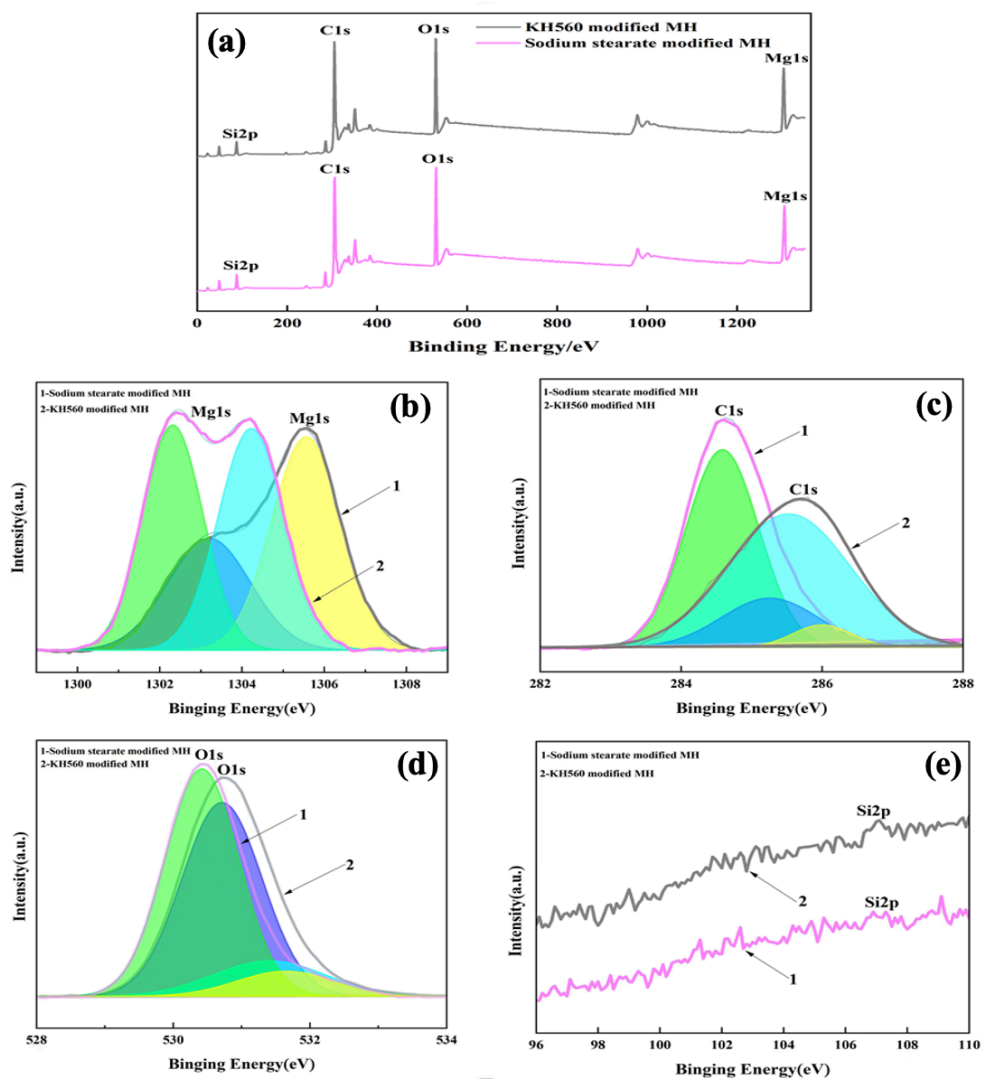


Fig. 9. XPS peak scanning pattern of modified MH

eV and 530.39 eV were observed to be higher than the standard binding energy at 529.95 eV, attributing to hydroxide species. This suggests that fracture occurrence along the dissociation plane of magnesium hydroxide, resulting in the disruption of -OH groups and a shift in the binding energy. Moreover, the Si2p spectrum (refer to Fig. 9e) could not be fitted during the modification process. The modification of sodium stearate results in a binding energy below the standard value of 103.26 eV, indicating that the binding energy of silicon on the surface of magnesium hydroxide is lower. These results further confirm that sodium stearate offers the most effective modification effects.

### 3.3. Flame retardancy of composite materials

Fig. 10 demonstrates that the addition of magnesium hydroxide to the polypropylene composite materials results in a delayed onset temperature of degradation ( $T_{0wt\%}$ ) compared to the pure polypropylene matrix. The initial decomposition temperature of pure polypropylene is 240°C, whereas for the polypropylene composites with flame retardants, the initial decomposition temperature exceeds 240°C. MH/PP composite modified with sodium stearate exhibits the highest initial decomposition temperature, thereby significantly improving the flame retardancy of the polypropylene material.

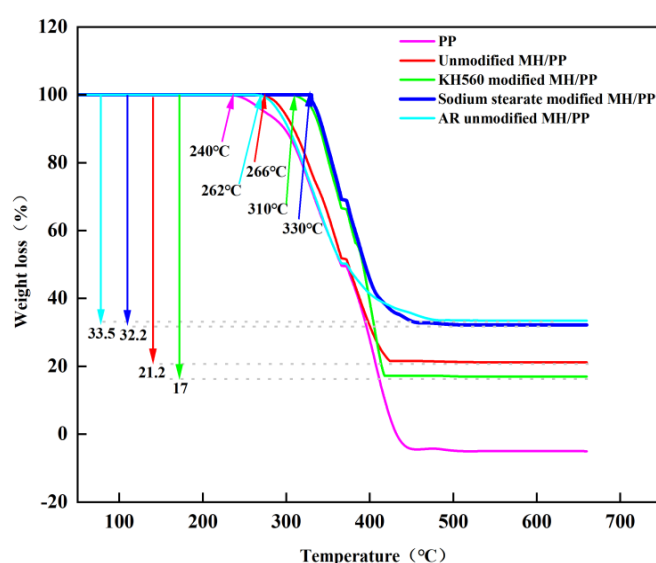


Fig. 10. TGA curves of PP and its composites

Given that the initial decomposition temperature of magnesium hydroxide is around 340°C, the addition of sodium stearate enhances the stability of magnesium hydroxide. The resulting magnesium hydroxide possesses lower polarity and stronger hydrophobicity, which facilitates better dispersion of modified magnesium hydroxide within the polypropylene composite. When polypropylene and magnesium hydroxide are mixed, the overall decomposition temperature of the composite material. However, as the temperature rises, the polypropylene composites gradually degrade. The pure polypropylene matrix degrades significantly higher than the flame retardant-incorporated components. It burns out completely without leaving any residual carbon within a short period. Including flame retardants in the polypropylene composites slows down the degradation rate and leaves a substantial amount of residual carbon even at a burning temperature of 650°C. Among the compositions, the AR MH/PP composite without modification exhibits the slowest degradation rate, with a residual carbon content of 33.5%. The residual carbon content of MH/PP composite modified by sodium stearate is 32.2%.

The Limiting Oxygen Index (LOI) test evaluates the flame retardancy of polymers by measuring the minimum concentration of oxygen required to sustain combustion within a material (Chen et al. 2009). Fig. 11 illustrates that the LOI of pure polypropylene is 18.5%. It does not meet any classification in the UL-94 vertical burning test, indicating that it is flammable. Adding different types of magnesium hydroxide increases the LOI of the polypropylene composites. Magnesium hydroxide promotes flame retardancy through endothermic decomposition, which results in the creation of stable magnesium

oxide and the release of water. Magnesium oxide is a protective oxide layer with high thermal stability. This layer helps prevent polymer degradation and improves the flame retardancy of polypropylene composites. The unmodified MH/PP composite exhibits an LOI of 23.5%, while the LOI value of the KH560-modified MH/PP composite is 23%. Moreover, the MH/PP composite modified with sodium stearate exhibits the highest LOI value of 25% and attains a V-1 classification in the UL-94 test, demonstrating excellent flame-retardant performance.

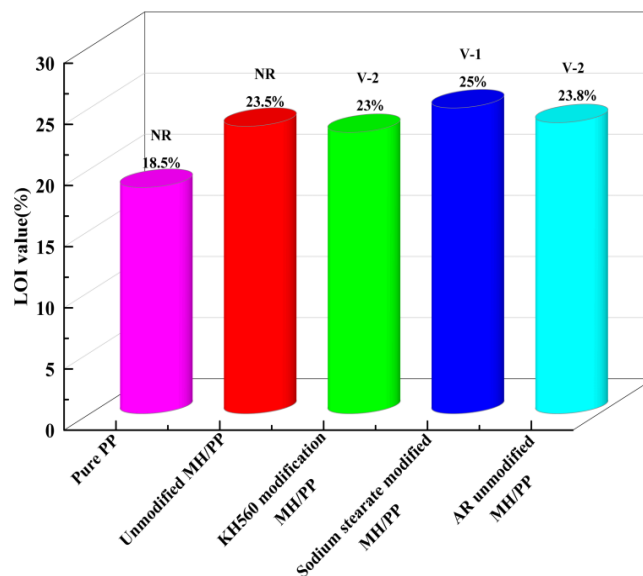


Fig. 11. Test results of LOI and UL-94 for PP and PP composites

PCFC and cone calorimetric experiments are thermal analysis methods that play an active role in conducting effective flammability studies. They are used to assess the flammability of materials, such as polymers (Rhoda et al. 2019). Cone calorimetry is considered the best method for analyzing the combustion behavior of polymers. It is based on monitoring the oxygen consumption of a polymer sample during constant heat flux irradiation. In general, pHRR (peak heat release rate), TTI (time to ignition), and THR (total heat release) are considered to be the key parameters for cone calorimetric analysis of flame-retardant properties of polymer materials. Of course, the longer the TTI, the higher the flame retardancy. Additionally, the lower the THR and pHRR values are, the greater the improvement in flame retardancy characteristics. (Henri et al. 2020). In general, the flammability of a material is characterized by the amount of heat released when the material is exposed to fire. The most important property measured from PCFC experiments is HRR.

Fig. 12a and Table 1 show that the peak heat release rate of unmodified magnesium hydroxide decreased by 71.01% compared to pure PP. The peak heat release rate of KH560-modified magnesium hydroxide reached 135.8 kW/m<sup>2</sup>, a decrease of 75.64% compared to the pure PP system. Additionally, the peak heat release rate of sodium stearate-modified magnesium hydroxide decreased by 87.1% compared to the pure PP system. The peak heat release rate of AR unmodified magnesium hydroxide decreased by 83.3% compared to pure PP. The rate of heat release is determined by the rate at which flammable volatiles are produced under a specific heat flux. The danger level of combustibles in real life mainly depends on the rate of heat release from the burning polymer. When the material is heated to its ignition temperature, the heat release rate of the polymer can be determined over time.

From the HRR curve, it can be observed that the peak heat release rate of the pure PP system during combustion exhibits a distinct, sharp, and narrow peak. This suggests that the combustion of PP primarily occurs in the gas phase, resulting in the rapid release of a significant amount of heat. Looking at the curve modified by magnesium hydroxide, it can be observed that there is no distinct peak in the curve. Instead, there is a flatter platform with lower intensity, and the peak time of heat release rate is delayed. This is because the dilution of flame chemistry occurs simultaneously with the suppression of gas phase flames. Magnesium hydroxide begins to decompose above 300 °C, resulting in the production of water. The presence of water dilutes the ratio of combustible gas to oxygen in the gas phase.

Additionally, this decomposition reaction absorbs a significant amount of heat, which cools the flame and further reduces combustion. Another byproduct of decomposition is magnesium oxide, which forms a thermal insulation layer on the surface of the polymer. This layer slows down the rate of pyrolysis, prevents heat from entering the material, and reduces the speed of combustion. The heat release rate and total heat release are also reduced.

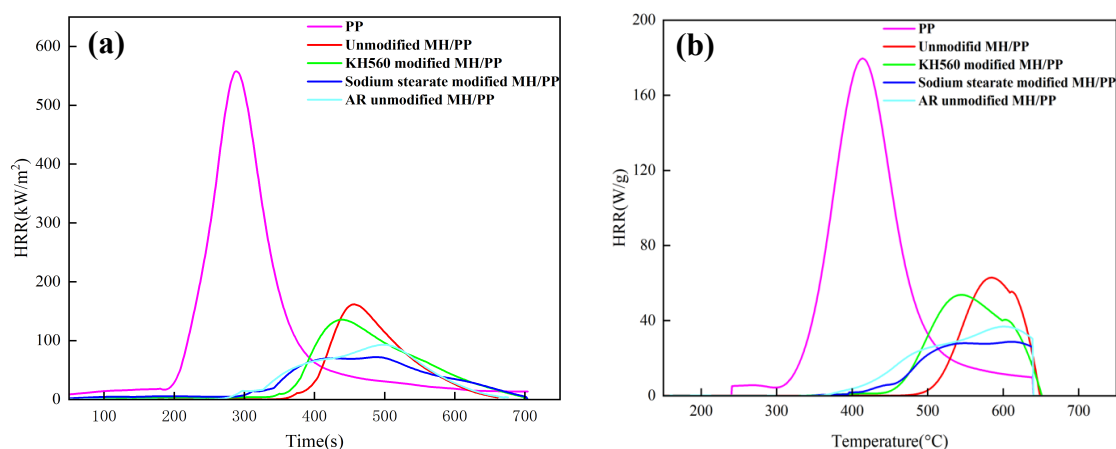


Fig. 12. Heat release rate (HRR) curves of samples measured using (a) cone calorimeter and (b) pyrolysis combustion flow calorimetry (PCFC)

Fig. 12b shows that the HRR curve of PP is narrow, due to a significant amount of heat being released in a short period of time. On the other side, the HRR curve containing magnesium hydroxide appears broad due to the strong condensed phase action of  $Mg(OH)_2$  crystals during the initial decomposition steps, resulting in a slower release of heat over a longer period of time.

Based on the HRR curve, it can be observed that the PHRR of PP decreased significantly after the addition of sodium stearate modified magnesium hydroxide. Additionally, the location of the heat release peak shifted noticeably, indicating that the addition of sodium stearate to magnesium hydroxide significantly improved its flame-retardant effect on PP.

Table 1. Results from cone calorimetry tests for different kinds of magnesium hydroxide polypropylene composites

samples	TTI (s)	THR (MJ/m <sup>2</sup> )	pHRR (kW/m <sup>2</sup> )	SPR (m <sup>2</sup> /s <sup>-1</sup> )
PP	94	63.4	557.5	0.013
Unmodified MH/PP	119	21.9	161.6	0
KH560 modified MH/PP	136	24.3	135.8	0
Sodium stearate modified MH/PP	167	23.8	71.9	0
AR unmodified MH/PP	144	19.1	93.1	0

### 3.4. Mechanical properties of composite materials

According to Fig. 13, the composites of MH/PP modified with sodium stearate exhibit the highest elongation at break, reaching 23.35%. In contrast, the modification of KH560 has a relatively minor effect on the toughness of the composite materials, while the unmodified magnesium hydroxide does not demonstrate any toughness (refer to Fig. 13a). This indicates the positive impact of sodium stearate modification on the toughness of the composite materials.

Furthermore, the addition of modifiers, such as sodium stearate and KH560, enhances the tensile strength of the MH/PP composites (refer to Fig. 13b). This improvement can be attributed to the facilitated interaction between magnesium hydroxide and polypropylene due to the inclusion of modifiers, leading to improved dispersion of magnesium hydroxide within the polypropylene matrix, ultimately elevating the tensile strength of the polypropylene composites. These findings highlight the

effectiveness of modifiers in enhancing the dispersion of magnesium hydroxide within the polypropylene matrix, thus enhancing the mechanical properties of the composite materials. This bears significant practical implications for developing high-performance MH/PP composites.

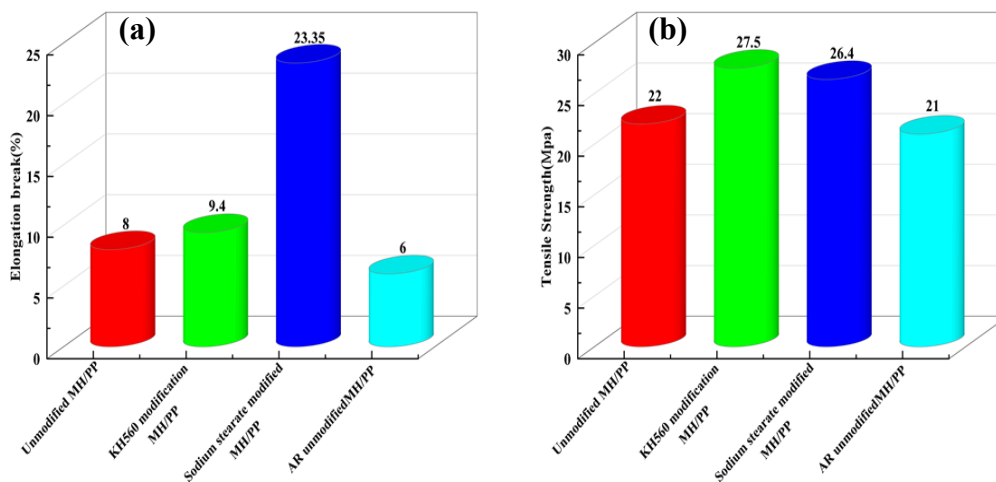


Fig. 13. Tensile properties of PP composites

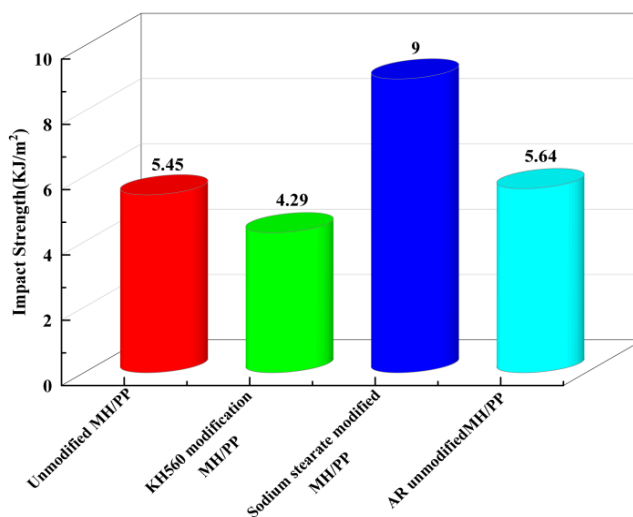


Fig. 14. Impact strength of PP composites

The impact strength data provided in Fig. 14 shows that the polypropylene composites with unmodified magnesium hydroxide exhibit a notched impact strength of 5.45 KJ/m<sup>2</sup>. The AR unmodified MH/PP composite with a notched impact strength of 5.64 KJ/m<sup>2</sup> exhibits only a minor variation when compared to the unmodified MH/PP composite. However, the impact strength of the KH560-modified MH/PP composite is 4.29 KJ/m<sup>2</sup>, indicating poor dispersion and compatibility when combined with polypropylene, resulting in a lower notched impact strength. Conversely, the MH/PP composite modified with sodium stearate exhibit a notched impact strength of 9 KJ/m<sup>2</sup>, indicating that the sodium stearate modification lowers the surface energy and polarity of the magnesium hydroxide particles, improving their hydrophobicity and facilitating their effective dispersion within the polypropylene matrix with good compatibility. Therefore, the addition of sodium stearate can enhance the notched impact strength of polypropylene composites, which is beneficial for using polypropylene composites as flame retardant additives in composite materials.

#### 4. Conclusions

In this work, we synthesized magnesium hydroxide with controllable processes and stable morphology via a simple hydration method, combined with the introduction of sodium stearate and KH560

modifiers. The structure and composition of magnesium hydroxide were confirmed by SEM, laser particle size analysis, XRD, FTIR, and XPS, and the flammability and compatibility of the polypropylene matrix were assessed with LOI, UL-94, tensile properties, and impact strength tests. Results revealed that sodium stearate as a modifier had the best modification effect on magnesium hydroxide. During the hydration process, introducing sodium stearate led to weak esterification of magnesium hydroxide, manifested as smaller and more uniform particle size, the contact angle reaching  $120.32^\circ$ , and a reduced surface free energy value of  $1.34\text{mN/m}$ .

This successful transition of magnesium hydroxide from being hydrophilic to hydrophobic facilitated improved dispersion. Among polypropylene composites, sodium stearate-modified magnesium hydroxide exhibited exceptional flame-retardant properties. It achieved the highest LOI value of 25%, UL-94 V-1 grade, and a residual carbon content of 32.2%. Additionally, the pHRR was reduced by 87.1%, THR was significantly reduced, and smoke emissions were non-existent. Furthermore, the mechanical properties of the magnesium hydroxide/polypropylene composite, modified by sodium stearate, showed a noticeable improvement. Elongation at break increased from 8% to 23.35%, and impact strength increased from  $5.45\text{KJ/m}^2$  to  $9\text{KJ/m}^2$ , with better toughness and strength. In conclusion, this study offers a stable approach to synthesizing hydrophobic, low-polarity, and highly compatible magnesium hydroxide through a modifier-guided hydration process—an advancement in the practical application of affordable, eco-friendly flame-retardant materials.

### Acknowledgments

This research was funded by the Natural Science Foundation of Hebei Province (Iron and Steel Union) (Grant No. E2022209127), the Science and technology research project of colleges and universities in Hebei Province (Grant No. CXY2023008).

### References

- MENSAH, R. A., SHANMUGAM, V., NARAYANAN S., RENNER, J. S., BABU, K., NEISIANY, R. E., FORSTH, M., SAS, G., DAS, O. 2022. *A review of sustainable and environment-friendly flame retardants used in plastics*. *Polymer Testing* 108, 107511.
- MOHAMMED, R., R. C. MOHAMMED. 2022. *Role of polymer-filler interaction on  $\text{Mg}(\text{OH})_2$  and aluminatrichydrate-loaded ethylene propylene diene monomer based polymer composite for high voltage insulation application*. *Journal of Applied Polymer Science* 139(20), 1-14.
- MUIRURI, J. K., J. C. C. YEO, Q. ZHU, E. YE, X. J. LOH, Z. B. LI. 2023. *Bacterial cellulose: Recent advances in biosynthesis, functionalization strategies and emerging applications*. *European Polymer Journal* 199, 112446.
- BROSTOW, W., S. LOHSE, A. T. LU. 2019. *Nano- $\text{Al}(\text{OH})_3$  and  $\text{Mg}(\text{OH})_2$  as flame retardants for polypropylene used on wires and cables*. *Emergent Mater* 2(1), 23-34.
- HE, W. T., P. A. SONG, B. YU, Z. P. FANG, H. WANG. 2020. *Flame retardant polymeric nanocomposites through the combination of nanomaterials and conventional flame retardants*. *Progress in Materials Science* 114, 100687.
- MORGAN, A. B., J. W. GILMAN. 2013. *An overview of flame retardancy of polymeric materials: application, technology, and future directions*. *Fire and Materials* 37(4), 259–279.
- JENO, G, A, J., R. RATHNA, E. NAKKEERAN. 2021. *Biological Implications of Dioxins/Furans Bioaccumulation in Ecosystems*. *Environmental Pollution and Remediation* 395-420.
- HENRI, V., L. FOUAD, M. MEHRSHAD, R. S. MOHAMMAD, D. PHILIPPE. 2020. *Flame retardant polymer materials: An update and the future for 3D printing developments*. *Materials Science & Engineering R144*, 100604.
- NEREA, P., X. L. QI, S. B. NIE, P. ACUÑA, M. J. CHEN, D. Y. WANG. 2019. *Flame retardant polypropylene composites with low densities*. *Materials* 12(1), 152.
- PARIDA, M, R., S. MOHANTY, M. BISWAL, S. K. NAYAK. 2022. *Influence of aluminum trihydrate (ATH) particle size on mechanical, thermal, flame retardancy and combustion behavior of polypropylene composites*. *Journal of Thermal Analysis and Calorimetry* 148(3), 807-819.
- ARZHAKOVA, O. V., A. A. DOLGOVA, A. YU. KOPNOV, A. YU. YARYSHEVA, A. L. VOLYNSKII. 2023. *Efficient Approach to the Preparation of Flame-Retardant Nanocomposite Polymeric Materials Based on High Density Polyethylene and Magnesium Hydroxide*. *Doklady Physical Chemistry* 510(2), 95-99.

- PILARSKA, A., M. WYSOKOWSKI, E. MARKIEWICZ, T. JESIONOWSKI. 2012. *Synthesis of magnesium hydroxide and its calcinates by a precipitation method with the use of magnesium sulfate and poly(ethylene glycols)*. Powder Technol. 235, 148–157.
- SIERRA-FERNANDEZ, A., L.S. GOMEZ-VILLALBA, O. MILOSEVIC, R. FORT, M.E. RABANAL. 2014. *Synthesis and morpho-structural characterization of nanostructured magnesium hydroxide obtained by a hydrothermal method*. Ceramics International 40(8), 12285–12292.
- ZHANG, H. Y., H. Q. WANG, H. Q. WANG. 2018. *Flame retardant mechanism and surface modification of magnesium hydroxide flame Retardant*. IOP Conference Series: Earth and Environment Science 170(3): 032028.
- LIANG, J. Z. 2017. *Tensile and flexural properties of polypropylene composites filled with highly effective flame retardant magnesium hydroxide*. Polymer Testing 60, 110–116.
- WANG, SEN., S. T. LIANG, K. S. WANG, J. C. LIU, J. LUO, S. G. PENG. 2023. *Enhanced flame retardancy, smoke suppression, and acid resistance of polypropylene/magnesium hydroxide composite by expandable graphite and microencapsulated red phosphorus*. Journal of Vinyl and Additive Technology 29(2), 395–409.
- ZHANG, F., Y. Y, FENG, W, FENG. 2020. *Three-dimensional interconnected networks for thermally conductive polymer composites: Design, preparation, properties, and mechanisms*. Materials Science and Engineering 142: 100580.
- LIU, W. P., H. XU, Z. X. WANG, X.M. WANG. 2019. *Adsorption of Water and Fatty Acids at Magnesium Hydroxide Surface from a MDS Perspective*. Surface Innovation 7(5), 1–12.
- PANG, H. C., J. W. YE, J. Q. LI, F. YA, Y. LIN, G. L. NING. 2008. *Study of modification of magnesiumhydroxide bonded with lauric acid and application in PE*. Sciencepaper Online 3(6), 415–418.
- XU, J., T. TANG, AND H. QU. 2011. *One-step wet synthesis andcharacterisation of hydrophobic magnesium hydroxide*. Advanced Materials Research 194–196, 633–637.
- YUAN, Y., X. CHU, G. DU, G. TANG, Z. Yin. 2010. *Surface modification of superfine magnesium hydroxide by silane coupling agent*. Funct. Mater. 41(7), 1186–1189.
- LAN, S. J., L. J. LI, D. F. XU, D. H. ZHU. 2016. *Surface modification of magnesium hydroxide using vinyltriethoxysilane by dry process*. Applied Surface Science 382 56–62.
- XING, Z. B., L. M. BAI, Y. X. MA, D. WANG, M. LI. 2018. *Mechanism of Magesium Oxide Hydration Based on the Multi-Rate Model*. Materials (11), 3–13.
- LIU, J. H., N. FENG, S. Q. CHANG, H. L. KANG. 2012. *Preparation and characterization of poly (glycidyl methacrylate) grafted from magnesium hydroxide particles via SI-ATRP*. Applied Surface Science 258(16), 6127–6135.
- WANG, T., D. W. YAO, G. Z. YIN, Y. JIANG, N. WANG, D. Y. WANG. 2023. *Gallic acid-iron complex modified magnesium hydroxide and its effect on flame retardancy of EVA*. Advanced Industrial and Engineering Polymer Research 6(2), 172–180.
- BHATT, P., S. CHATTOPADHYAY, K. P. MISRA, D. MADAN, N. HALDER. 2021. *Effect of temporal pH variation of the reaction mixture on Mg (OH)<sub>2</sub> morphology precipitated from an aqueous Mg(NO<sub>3</sub>)<sub>2</sub>-NaOH system*. Advanced Powder Technology 32(7), 2289–2299.
- TANG, X. J., Z. Y. DU, Y. M. ZHU, P. F. LIU, X. Y. LI, X. L. XU, Y. Z. ZHAO, H. B KUANG. 2020. *Correlation between microstructure and dissolution property of magnesium hydroxide synthesized via magnesia hydroxylation: Effect of hydration agents*. Journal of Cleaner Production 249(C), 119371.
- LI, N., Z. LI, Z. Q. LIU, Y. X. YANG, Y. C. JIA, J. S. LI, M. WEI, L. J. LI, D. Y. WANG. 2022. *Magnesium hydroxide micro-whiskers as super-reinforcer to improve fire retardancy and mechanical property of epoxy resin*. Polymer Composites 43(4), 1996–2009.
- MASTRONARDO, E., L. BONACCORSI, Y. KATO, E. PIPEROPOULOS, M. LANZA, C. MILONE. 2017. *Strategies for the enhancement of heat storage materials performances for MgO/H<sub>2</sub>O/Mg(OH)<sub>2</sub> thermochemical storage system*. Applied Thermal Engineering 120, 626–634.
- ZAHRA, R., R. NAGHIZADEH, A. ZOLRIASATEIN, S. BAGHERI, C. MELE, C. E. Corcione. 2023. *Hydrophobic, Mechanical, and Physical Properties of Polyurethane Nanocomposite: Synergistic Impact of Mg (OH)<sub>2</sub>and SiO<sub>2</sub>*. Polymers 15(8), 1916.
- ZHANG, M. Y., J. X. LYU, Y. F. ZUO, X. G. LI, P. LI. 2023. *Effect of KH560 concentration on adhesion between silicate modified poplar and waterborne varnish*. Progress in Organic Coatings 174(12), 107267.
- NYQUIST, R. A. 1998. *Book Reviews: Infrared and Raman Spectra of Inorganic and Coordination Compounds, Infrared and Raman Spectra of Inorganic and Coordination Compounds*. Applied Spectroscopy 52(3), 124A–125A.
- RYO, K., T. MASATO, R. JUNICHI. 2021. *Fourier-transform infrared and X-ray diffraction analyses of the hydration reaction of pure magnesium oxide and chemically modified magnesium oxide*. RSC Advances 11(39), 24292–24311.

- SONG, T., F. F. GAO, X. DU, X. G. HAO, Z. LIU. 2023. *Removal of boron in aqueous solution by magnesium oxide with the hydration process*. *Colloids and Surfaces A: Physicochemical and Engineering Aspects* 131211.
- GUO, L., F. ZHANG, L. SONG, R. C. ZENG, S. Q. LI, E. H. HAN. 2017. *Corrosion resistance of ceria/polymethyltrimethoxysilane modified magnesium hydroxide coating on AZ31 magnesium alloy*. *Surface&Coatings Technology* 328, 121-133.
- LI, Y. Y., S. P. WU, Y. DAI, L. PANG, Q. T. LIU, J. XIE, D. Z. KONG. 2018. *Investigation of sodium stearate organically modified LDHs effect on the anti-aging properties of asphalt binder*. *Construction and Building Materials* 172, 509-518.
- LI, S. W., J. H. WANG, S. G. WEN, Y. B. CHEN. 2021. *Synergistic effect of aluminum diethylphosphinate/sodium stearate modified vermiculite on flame retardant and smoke suppression properties of amino coatings*. *RSCADVANCES* 11, (54), 34059-34070.
- CHEN, X. L., J. YU, S. Y. GUO, S. J. LU, Z. LUO, M. He. 2009. *Surface modification of magnesium hydroxide and its application in flame retardant polypropylene composites*. *Journal of Materials Science* 44(5), 1324-1332.
- RHODA, A., M. X. QIANG, A. O. SOLOMON, J. CONG, B. M. GEOFFREY. 2019. *Correlation analysis of cone calorimetry and microscale combustion calorimetry experiments*. *Journal of Thermal Analysis and Calorimetry* 136:589-599.
- HENRI, V., S. RODOLPHE, T. AURÉLIE, O. BELKACEM, R. S. MOHAMMAD, B. GÜNTER. 2020. *Halloysite nanotubes (HNTs)/polymer nanocomposites: thermal degradation and flame retardancy*. *Clay Nanoparticles*, 67-93.